

EFFECTS OF FEMORAL NECK GEOMETRY ON STRESS DISTRIBUTION: IMPLICATION FOR STRESS FRACTURE RISK

Liming Voo, Mehran Armand

Biomechanics and Injury Prevention
Johns Hopkins University Applied Physics Laboratory
Laurel, Maryland

INTRODUCTION

Stress fracture of the femoral neck can be classified as compression and tension fractures. Compression stress fracture occurs at the inferior surface of the femoral neck. It is generally stable and requires only resting without need for surgical intervention. Tension stress fracture of the femoral neck, on the hand, initiates at the superior surface of the femoral neck and causes a transverse fracture across the neck. It is generally unstable and requires immediate surgical intervention. Stress fractures of the femoral neck are particularly serious and difficult to diagnose, requiring relatively expensive imaging modalities such as MRI and bone scans [1-7]. Delays in diagnosis can allow a relatively minor stress fracture to advance to a completed femoral neck fracture, which is a catastrophic event in a young soldier. Even with emergency surgery, the hip joint will often suffer from osteonecrosis, or death of the femoral head [2,3,5,6]. This not only precludes the soldier from returning to military training, but results in a medical discharge with lifelong disability and liability. Identifying the specific characteristics and loading conditions in the femur of the individuals who are more prone to tension, rather than compression, stress fracture of the femur can help early diagnosis of this injury and prevent more catastrophic disability.

This study examines the effects of femoral neck geometry on its stress distribution under a simulated loading condition of single leg stance phase during normal walking and running using finite element analysis.

MATERIALS AND METHODS

An algorithm was developed to extract the geometry of a normal healthy male femur from three-dimensional computed tomography (CT). The gray scale and density values of the CT images of the proximal femur bone were calibrated. Edge extractions were performed for the outer boundaries of the femur using the re-sliced sections along the femur shaft and neck axis. The bony outlines were approximated by a series of ellipses using non-linear least-square fit of an elliptical equation to the outlines found from the edge extractions. The marrow/cancellous and the cortical/cancellous boundaries were

determined using a series of inner ellipses inside the outer ellipses. These inner boundaries were calculated to satisfy a set of constraint equations for maintaining equal cross-sectional moment of inertia and area between the model and the calculated CT density data.

A finite element mesh was created based on the geometry described above using an automatic procedure in the I-DEAS program. The volume inside the inner cortex was filled with brick elements representing cancellous bone. The cortical shell included two layers of brick elements. The model representing the original anatomy of the proximal human femur contains 15,360 brick elements with 15,633 nodes. Material properties of the bone were assumed to be isotropic and linear elastic, and were based on similar data reported in the literature. The modulus of elasticity was 17 GPa for cortical bone and 1.5 GPa for cancellous bone. Poisson's ratio for the bone tissue was 0.33.

Three geometric parameters of the femoral neck were investigated in this study: cortex thickness, length and neck-shaft angle. The thickness of the superior cortex was reduced by 2 mm while that of the inferior cortex was increased by 2 mm in the femoral neck region to create the Thickness Model. A model representing a longer femoral neck was created by widening the distance between the adjacent cross-sections in the femoral neck region with an accumulated total increase of 15 mm (Long-neck Model). Another model representing a smaller neck-shaft angle was produced by increasing the angle between adjacent cross-sections in the region that includes the greater trochanter and neck, with an accumulated total increase of 15 degrees (Small-angle Model).

Stress analyses were performed on all three finite element models (the original model plus three geometric variations). Kinematic constraints were applied to the most distal part of the shaft. A single distributed vertical force of 2500 N was applied to the superior surface of the femoral head. This loading condition was adapted to simulate the force transmitted through the hip joint when a person was in the stance phase of normal walking with no action of the abductor muscles. Stress analyses, and pre- and post-processing were performed using the I-DEAS program.

RESULTS AND DISCUSSIONS

The stress distribution of the models were expressed in terms of von Mises stress (Figures 1-3). For the normal model (Figure 1), maximum stress occurred at the inferior root of the femoral neck. The maximum stress in the superior surface of the neck was approximately one third of that in the inferior surface. The stress in this region was increased by approximately 65% and was only approximately 16% less than that in the inferior neck region in the longer neck model (Figure 2). The overall maximum stress location however, shifted to the inferior lateral corner of the model boundary.

An even higher relative stress was sustained in the superior neck cortex in the small angle model (Figure 3). The stress in the superior neck cortex was increased by approximately 85% compared to that in the original model and was only about 10% less than the overall maximum. Changing the cortical thickness do not significantly alter the stress distribution in the femoral neck.

Previous biomechanical studies have determined that the ultimate strength of femoral cortical bone is approximately 45% higher in compression than in tension [8]. Other studies have show that the neck length can range by more than 30mm and neck-shaft angle by more than 30 degrees in a normal population [9]. The results from the present study suggest that a normal person with a longer neck and lower neck-shaft angle in his/her femur can have a higher risk for the unstable tension stress fracture of the femoral neck.

CONCLUSION

This analytical study demonstrated that bone geometry could be a critical factor in fracture risk for a human femoral neck. In a normal femur under normal walking or running conditions, the compressive stress generally predominates in the femoral neck area; thus stress fracture of the femoral neck is not likely to occur. However, a person whose femoral neck is longer and/or more horizontal is at a considerably higher risk for stress fracture of the unstable fracture type as demonstrated in this study.

ACKNOWLEDGMENT

This work was supported in part by the Independent Research and Development Grant in Biomedicine from the Johns Hopkins University Applied Physics Laboratory.

REFERENCES

1. Boden BP, Speer KP. 1997, "Femoral stress fractures," Clin Sports Med, 16(2):307-17.
2. Boden BP and Osbahr DC, 2000, "High-risk stress fractures: evaluation and treatment," J Am Acad Orthop Surg, 8(6):344-53
3. Clough TM. 2002, "Femoral neck stress fracture: the importance of clinical suspicion and early review," Br J Sports Med. 36(4):308-9.
4. Egol KA, Koval KJ, Kummer F, Frankel VH. 1998, "Stress fractures of the femoral neck," Clin Orthop, 34(8):72-8
5. Johansson C, Ekenman I, Tornkvist H, Eriksson E. 1990, "Stress fractures of the femoral neck in athletes: The consequence of a delay in diagnosis," Am J Sports Med. 18(5):524-8.
6. Muldoon MP, Padgett DE, Sweet DE, Deuster PA, Mack GR. 2001, "Femoral neck stress fractures and metabolic bone disease," J Orthop Trauma. 15(3):181-5.
7. Volpin G, Hoerer D, Groisman G, Zaltzman S, Stein H. 1990, "Stress fractures of the femoral neck following strenuous activity.," J Orthop Trauma. 4(4):394-8.
8. Reilly DT and Burstein AH. 1975, "The elastic and ultimate properties of compact bone tissue," J Biomech, 8:393-405.

9. Mahaisavariya B, Sitthiseripratip K, Tongdee T et al., 2002, "Morphological study of the proximal femur: a new method of geometrical assessment using 3-dimensional reverse engineering," Med Eng & Physics, 24:617-622.

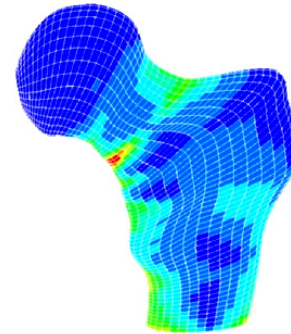


Figure 1. Stress distribution of the original femur model

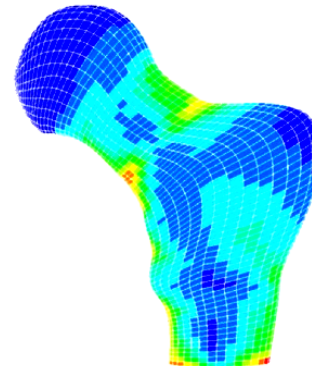


Figure 2. Stress distribution of the proximal femur model with a longer neck

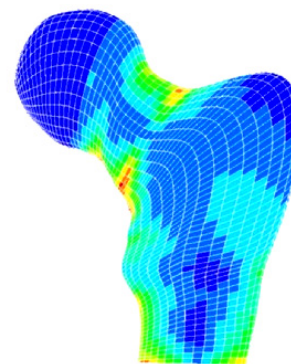


Figure 1. Stress distribution of the proximal femur model with a lower neck-shaft angle